International Journal of Environmental Science and Technology (2024) 21:7717–7732
https://doi.org/10.1007/s13762-024-05484-0

ORIGINAL PAPER

Enhanced treatment of oily wastewater through modified magnetic seeds for magnetic flocculation

L. Zhang[1] · B. Wang[1] · Q. Zhang[1]

Received: 17 September 2023 / Revised: 21 November 2023 / Accepted: 23 January 2024 / Published online: 28 February 2024

Abstract

This study delves into assessing the effectiveness of modified magnetic seeds in treating oily wastewater through magnetic flocculation. Initially, the research focuses on characterizing the magnetic seeds' properties and evaluating their oil adsorption capabilities pre- and post-modification. The investigation identifies a correlation between the adsorption process and the second-stage kinetic magnetic seed model as well as the Langmuir model, both before and after modification. Moreover, the study highlights the enhanced adsorption capacity of modified magnetic seeds for chemical oxygen demand in comparison with conventional ones. Interestingly, both types of seeds display a closer conformity with the Freundlich adsorption isotherm model concerning their oil adsorption behaviors. In the magnetic flocculation process, polymerized aluminum chloride serves as the flocculant at a specific concentration in conjunction with magnetic seeds. Optimal treatment conditions involve maintaining a particular water temperature and pH level. These conditions facilitate a chemical oxygen demand removal rate of 75.5% and an impressive 93.2% efficiency in removing oil content. As a result, utilizing modified magnetic seeds exhibits substantial potential in degrading pollutants within oily wastewater treatment. This approach not only enhances adsorption capabilities when combined with magnetic flocculation but also provides valuable theoretical insights into treating oily wastewater via magnetic flocculation.

Keywords Adsorption kinetics · Chemical oxygen demand · Magnetic flocculation · Modified magnetic seeds · Oil removal efficiency

Introduction

Water is a critical resource essential for human survival and various industrial operations, often found in conjunction with oil. With the continuous expansion of oil exploration and production, the volume of oilfield wastewater has dramatically increased. This wastewater is notably complex, characterized by elevated concentrations of organic compounds and contaminants associated with petroleum (Liu et al. 2013). The consequences of neglecting proper treatment or directly releasing these effluents into the environment are severe, resulting in irreversible ecological damage and posing substantial health hazards. Therefore, the efficient treatment of oilfield wastewater is paramount. It serves the dual purpose of meeting the criteria for secondary oil recovery water and aligning with national discharge standards (Li et al. 2015).

Magnetic flocculation technology has emerged as a progressive water treatment method, complementing traditional flocculation processes by employing magnetic seeds as carriers (Wang et al. 2014). Currently, Fe_3O_4 is a common magnetic adsorbent with good adsorption properties and is widely used. Surface functionalization of magnetic seeds primarily involves the use of inorganic materials, artificial organic polymers, and natural extracts (Zhao et al. 2018). These modified magnetic seeds play a pivotal role in enhancing flocculation efficiency. They contribute to the formation of more compact and heavier aggregates, thereby improving decontamination capabilities and sedimentation rates (Liu et al. 2018; Pinto et al. 2018).

Numerous studies have delved into the application of magnetic seeds across diverse contexts. Researchers studied the synthesis and structure of ferroferric oxide magnetic

Editorial responsibility: Q. Aguilar-Virgen.

✉ B. Wang
18202460111@163.com

[1] School of Municipal and Environmental Engineering, Shenyang Jianzhu University, Shenyang, China

nano-particles and their influence on the structure, optical and magnetic properties of new polymethyl methacrylate/polyaniline composite materials for electromagnetic and optical applications. The properties of ferroferric oxide were studied, evaluated, and eventually applied to magnetoelectric devices (Elamin et al. 2022). Many studies have been reported on magnetic Fe_3O_4 particles coating with organic materials as adsorbent for metal removal, such as chitosan and polyacrylamide (Liu et al. 2009a, b; Hong et al. 2007). Numerous widely modified the surface of Fe_3O_4 magnetic particles with organic magnetic seeds through ethanol and stearic acid, resulting in a remarkable 96.7% oil removal rate from oil-contaminated deep well groundwater. Someone synthesized nano-Fe_3O_4 with polymerized aluminum chloride and employed the modified magnetic seeds to treat Microcystis aeruginosa (Jiang et al. 2010). Several researchers harnessed ribose to modify the Fe_3O_4 surface, thus creating algae with the capability to eliminate algae from water (Liu et al. 2009a, b). Others fabricated a magnetic adsorbent from antigorite, bentonite, and iron oxide (ABI), showing excellent adsorption performance for both positively and negatively charged contaminants (Farahat et al. 2022). In addition, a magnetic COF adsorbent was made with abundant heteroatoms acting as effective adsorption sites. The adsorbent has good adsorption performance for Pb (II), with a removal rate of 95.64% at 10 min and a maximum adsorption capacity of 411.80 mg g^{-1}. According to the Zeta potential and XPS analysis, N and S on the surface of the adsorbent interact with Pb (II) through electrostatic attraction and chelation (Wang et al. 2023). What is more, porous carbon has excellent adsorption capacity and stability among all adsorption materials, so it has been used widely as adsorption materials (Singh et al. 2021; Shen 2022). Magnetic carbonaceous adsorbents were prepared from nano-Fe_3O_4 ball-milled biochar (BC) and activated carbon (AC), and their ability to adsorb methylene blue (MB) in water was evaluated and compared (Li et al. 2020). Besides, through the preparation of $MnFe_2O_4$-supported activated carbon magnetic adsorption materials ($MnFe_2O_4$@AC), which was used for the adsorption removal of acetochlor in water medium, the adsorption capacity of 0.2 g L^{-1} adsorbent at 25 °C was about 226 mg g^{-1} (Wang et al. 2021).

Coagulants and magnetic materials stand as pivotal elements in the magnetic coagulation process. Over time, coagulants have undergone continuous research and development, resulting in a variety of types available today. A prevailing direction in this realm emphasizes cost-effectiveness, low toxicity, and high efficiency. Inorganic high-molecular-weight coagulants exhibit notable dirt removal capabilities and possess high relative molecular weight, yet their toxic and corrosive nature is a concern. Conversely, synthetic organic high-molecular-weight coagulants offer advantages in coagulation with minimal influence from treatment conditions and reduced sludge production, but their cost tends to be higher. Additionally, residual monomers in high-molecular-weight polymers pose risks, including gene mutation, abnormal growth, and carcinogenic potential. In contrast, non-toxic natural coagulants present an eco-friendly alternative, devoid of secondary pollution risks. However, they often exhibit lower coagulant activity and might not yield optimal results when used independently. Thus, a strategic combination of these two coagulant types can significantly enhance treatment efficacy.

Unmodified magnetic iron oxide faces challenges in air due to its susceptibility to oxidation and agglomeration, diminishing the stability and dispersibility of the magnetic phase. Additionally, its limited specific surface area restricts its efficacy in purifying contaminated wastewater. However, through modification or surface treatment, the stability and specific surface area of Fe_3O_4 can be substantially enhanced. Material modification involves altering a material's surface morphology and structural composition through specific physical or chemical reactions to achieve desired modifications. This alteration significantly enhances the properties of modified magnetic materials in several aspects, including improved dispersibility, chemical stability, surface hydrophobicity/hydrophilicity, and biocompatibility.

In this experiment, our objective is to augment the removal efficiency of organic pollutants. We aim to achieve this by surface-modifying commonly used magnetic seeds. The assessment includes scanning electron microscopy (SEM), specific surface area pore analysis for comparing morphological and pore structural properties (Ma et al. 2003), X-ray diffraction (XRD), and vibrating-sample magnetometry (VSM). The study meticulously examines surface morphology, adsorption kinetics, and adsorption isotherms (Sharma and Lee 2017). It juxtaposes the performance and mechanisms of modified magnetic seeds against conventional ones in treating oily wastewater. Specifically, we focus on reducing chemical oxygen demand (COD) and oil concentration in raw water samples. Additionally, we explore the effects of various combinations of magnetic seed dosages, flocculant polymerized aluminum chloride (PAC), and coagulant aid polyacrylamide (PAM) on oily wastewater treatment efficacy. Through determining the optimal treatment combination and employing the single-factor method to control magnetic seed dosage, flocculant PAC concentration, and coagulant PAM concentration for both ordinary and modified magnetic seeds, we analyze the impact of individual factors on oily wastewater treatment. This comprehensive investigation aims to compare the treatment efficiency of two magnetic seeds, establish optimal conditions for the magnetic flocculation stage, and provide significant research insights. It furnishes a robust theoretical framework and experimental data crucial for oilfield-produced water

treatment, advancing high-efficiency pollutant removal practices.

The research was conducted at the Liaohe River Basin Water pollution Prevention and Control Research Institute from February 2023 to September 2023, Liaoning Province, China.

Materials and methods

Test equipment

The experimental materials encompassed raw water samples with a pH of 7, containing 1527 mg/L COD and 63 mg/L oil. The experimental apparatus and instruments utilized encompassed a UV–Vis spectrophotometer (SHANGHAI METASH INSTRUMENTS CO., LTD., China), an electronic balance (Fuzhou Huazhi Scientific Instrument Co., Ltd., USA), a precision acidity meter (Shanghai Leici Precision Instrument Co., Ltd., China), a specific surface area pore analyzer (Micromeritics Instruments Corporation., China), a blast drying oven (Shanghai Kuntian Laboratory Instrument Co., Ltd., China), a magnetic stirrer (Shanghai Meiyingpu Instrument and Meter Manufacturing Co., Ltd., China), a scanning electron microscope (Beijing Yi Cheng Heng Da Technology Ltd., China), as well as various testing materials and chemicals including potassium dichromate ($K_2Cr_2O_7$), potassium aluminum sulfate ($Kal(SO_4)_2$), ammonium molybdate($(NH_4)_2MoO_4$), sodium hydroxide (NaOH), nitric acid (HNO_3), hydrochloric acid (HCl), sodium chloride (NaCl), acetic acid, absolute alcohol purchased from Sinopharm Chemical Reagent Co., Ltd. (China). Ferroferric oxide was purchased from Jinan Zhiding Welding Material Co., Ltd. (China). The primary objective of this experiment was to perform surface modification on conventional magnetic seeds with the aim of treating petroleum and organic pollutants present in oily wastewater through the application of magnetic flocculation.

Magnetic seed preparation method

Fifty grams of Fe_3O_4 was weighed and immersed in 500 mL of 2% hydrochloric acid for a period of 2.5 h. Subsequently, 100 g of $FeCl_3$–$6H_2O$ was introduced to 1 L of water and thoroughly stirred to ensure complete dissolution of the iron salt. The Fe_3O_4 was separated from the hydrochloric acid solution and added to the iron salt solution. The pH was adjusted to 8–9 using a 1 mol/L NaOH solution with vigorous stirring, followed by slow-speed stirring for 1.5 h. The mixture was then subjected to a water bath at 100 °C for 40 min. The resulting mixture was filtered to obtain a solid phase, which underwent repeated washing with deionized water. The washed solid phase was subsequently dried in a blast oven at 110 °C for 5 h, resulting in the modified magnetic seed. The final weight of the modified seed was recorded as 74.8 g and was stored in a hermetically sealed container.

Characterization of magnetic seeds

The morphology of both plain and modified magnetic seeds was observed through scanning electron microscopy (SEM). Furthermore, the pore size distribution of both types of seeds was analyzed using the density functional theory (DFT) method to ascertain any alterations in pore dimensions.

Adsorption mechanism experiment

Adsorption kinetics

Two 500-mL conical flasks were prepared, each containing 200 mL of extracted oil at the same concentration and water. In each flask, 1 g of ordinary or modified magnetic seeds was introduced. The water samples were subjected to agitation at room temperature with a stirring speed of 200 r/min. Samples were extracted at intervals of 0, 1, 2, 3, 5, 10, 15, 20, 30, 40, and 50 min to assess the COD and oil content. The quasi-primary adsorption kinetic model, quasi-secondary adsorption kinetic model, and internal diffusion model fitting experiments were conducted successively (Njoku et al. 2014; Shin et al. 2011, Zhang et al. 2019).

Adsorption isotherms

Different containers were prepared, each containing 200 mL of oily solution with varying oil concentrations (5 mg/L, 10 mg/L, 15 mg/L, 20 mg/L, 25 mg/L, and 30 mg/L). A gram of ordinary or modified magnetic seed was added to each container. The solutions were stirred at 200 r/min for 60 min at room temperature using a thermostatic shaker. The resulting adsorption isotherms were generated by fitting data to two adsorption isotherm models (Langmuir 1918).

Experimental design

In this experiment, the flocculant polymerized aluminum chloride (PAC) was added and stirred at 200 r/min for 1 min. Subsequently, surface-modified magnetic powder was introduced, and stirring was maintained for an additional 1 min. The coagulant aid PAM was then added and stirred at 100 r/min for 2 min, followed by a 7-min settling period. The supernatant was extracted to determine the concentrations of COD and oil in the water samples. Under consistent conditions, the effects of various combinations of flocculant PAC, modified magnetic seeds Fe_3O_4, and coagulant aid PAM on the removal efficacy of COD and oil in the oily wastewater

were assessed to establish the optimal treatment combination. In the single-factor test, conditions such as magnetic seed dosage, flocculant concentration, coagulant aid concentration, and initial pH were varied, ultimately culminating in the determination of oil content rate and COD.

Results and discussion

Characterization

SEM analysis

Scanning electron microscope (SEM) images of both conventional and modified magnetic seeds were captured at a magnification of 2 microns. The ordinary magnetic seeds showcased a primarily spherical shape, boasting small particle size and excellent dispersion. Conversely, the modified magnetic seeds exhibited an irregular, granulated morphology, characterized by varied particle sizes, notably larger particles, and rugged surfaces marked by numerous tiny pores. This distinct contrast in morphology arises from the iron oxide layer present on the surface of the modified seeds, causing a significant transformation in their surface topography. The porous, rough, and heterogeneous nature of the modified magnetic seeds established the groundwork for the subsequent experiments (Fig. 1a, b).

Specific surface area and pore size distribution analysis

The analysis indicated that the pore sizes of the modified magnetic seeds predominantly fell within the range of 2–5 nm, signifying a substantial decrease in pore size compared to the conventional magnetic seeds (Fig. 2a, b).

Furthermore, the average pore volume of ordinary magnetic seeds measured 0.00169 cm^3/g, while that of the

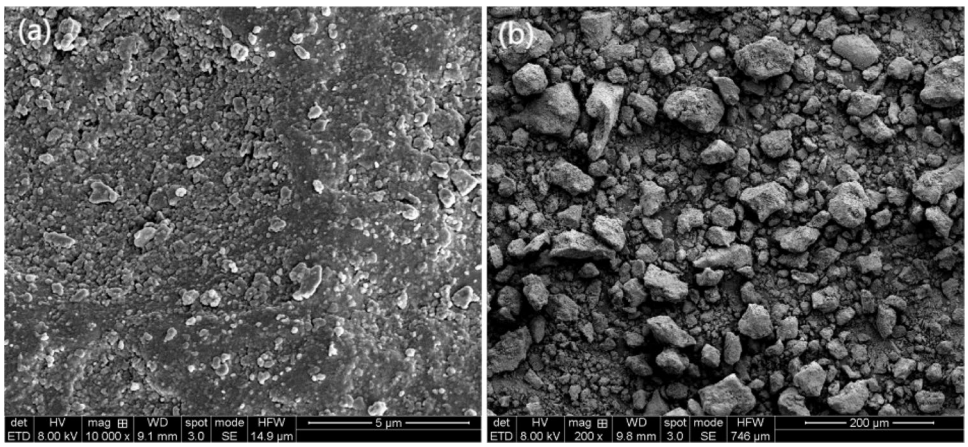

Fig. 1 Magnetic seeds (**a**) and modified magnetic seeds (**b**)

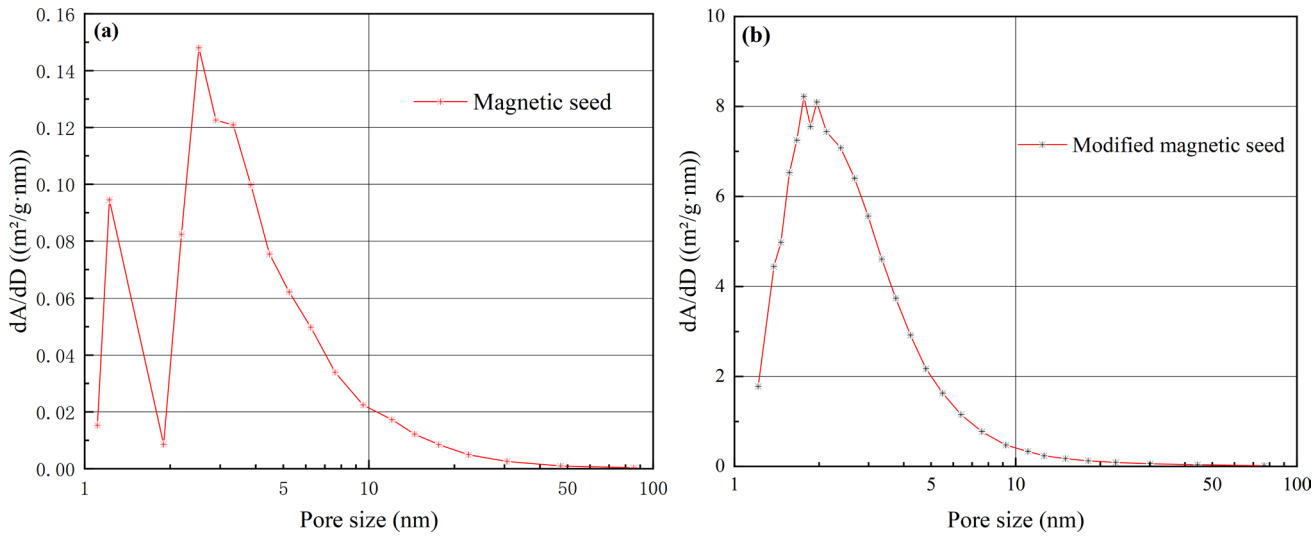

Fig. 2 Pore size distribution of ordinary magnetic seeds (**a**) and pore size distribution of modified magnetic seeds (**b**)

modified magnetic seeds was calculated at 0.04792 cm^3/g. The augmented pore volume in the modified magnetic seeds renders them highly effective for the adsorption of pollutants from water (Table 1).

XRD analysis

The characteristic peaks of the modified magnetic seeds are observed at $2\theta = 30.51°$, 35.48°, 43.29°, 57.09°, and 62.56°, well indexed to (220), (311), (400), (511), and (440) reflections of Fe_3O_4, respectively. XRD pattern confirms the pure formation of Fe_3O_4 without any presence of other Fe species like Fe_2O_3 and FeO. Comparatively, the diffraction spectrum of Fe_3O_4 in ordinary magnetic seeds displays weak peak intensity due to the crystal plane decrease attributed to smaller particle size and smoother surface, resulting in weaker or even absent trace diffraction peaks. Upon modification of the ordinary magnetic seeds, there is a noticeable increase in peak height, sharpening of peak shapes, enhanced resolution, and the emergence of clearer trace diffraction peaks. Analysis of these strong Fe_3O_4 peaks indicates that the modification primarily results in increased specific surface area and pore structure. This augmentation contributes to superior adsorption performance when pollutants interact with the Fe_3O_4 crystal planes. The enhanced crystallinity of the modified magnetic seeds demonstrates its improved effectiveness. Comparison of the characteristic diffraction peak intensities between the modified and ordinary magnetic seeds indicates the effective combination of modified magnetic seeds with the flocculant, forming modified magnetic flocs. Consequently, this leads to a reduction in the content of individual components (Fig. 3).

VSM analysis

The hysteresis lines of the magnetic flocculants were measured, respectively, which showed a typical "S" curve, indicating that the coercivity values were low and the flocculants had good superparamagnetism. The saturation magnetization strength (M) was 58.91 emu-g and 11.43 emu-g, respectively, which obviously showed that the modified magnetic seeds were better than the common magnetic seeds. During the flocculation process, the modified magnetic seeds were wrapped by a large number of flocs to form stable magnetic flocs, which could accelerate the settling speed and reduce the settling time under the action of the applied magnetic field (Fig. 4).

Table 1 Comparison of pore capacity before and after modification of Fe_3O_4

Magnetic seeds	Pore volume by single-point method (cm^3/g)	T-planar microporosity (cm^3/g)
Magnetic seeds	0.002847	0.000526
Modified magnetic seeds	0.092874	0.002976

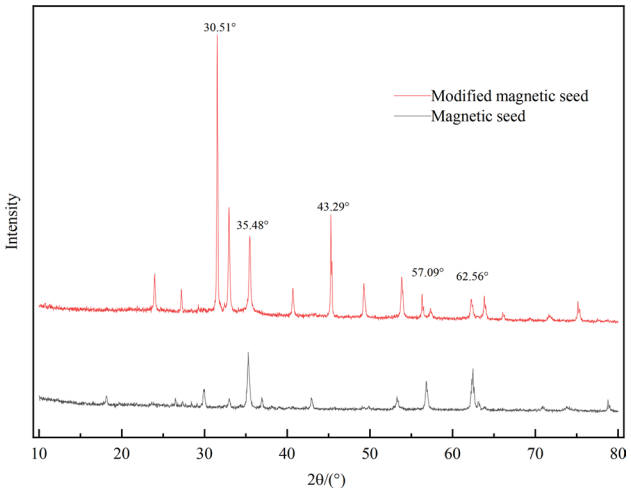

Fig. 3 Characterization results of XRD spectrum of magnetic seeds

COD adsorption experiment

Both conventional and modified magnetic seeds displayed a swift increase in COD adsorption within the initial 5 min, followed by a gradual decrease in the rate of increase. Adsorption ultimately stabilized after 15 min. At the 15-min mark, the equilibrium adsorption amount for conventional magnetic seeds plateaued at 36.15 mg. Conversely, the modified magnetic seeds reached equilibrium after 12 min, showcasing an adsorption capacity of 48.37 mg. Evidently, adsorption increased progressively over time. This outcome

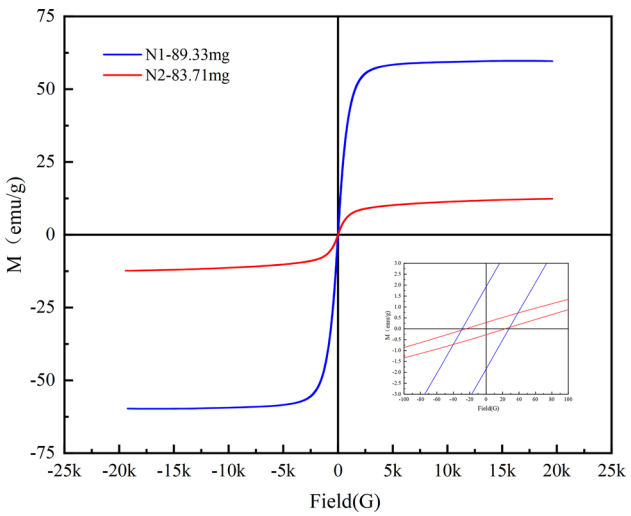

Fig. 4 Magnetic hysteresis curve of magnetic seeds

underscores the enhanced COD adsorption capability of the modified magnetic seeds after complete exposure to organic pollutants. This improvement is attributed to their amplified specific surface area and finer pore structure, providing superior performance compared to their conventional counterparts (Fig. 5a–c).

The experimental data concerning COD adsorption by both conventional and modified magnetic seeds did not conform to the trend predicted by the internal diffusion model, indicating its inadequacy in describing the COD adsorption process accurately. However, the quasi-first-order and quasi-second-order adsorption kinetic models showed excellent fits for the adsorption behavior of COD by both types of magnetic seeds. For conventional magnetic seeds, the quasi-first-order and quasi-second-order models exhibited correlation coefficients (R^2) of 0.93 and 0.97, respectively. Similarly, for modified magnetic seeds, the correlation coefficients (R^2) were measured at 0.95 and 0.99. Particularly noteworthy was the quasi-second-order model's higher R^2 value, suggesting an enhanced fitting effect. The determination of equilibrium concentration (Q_e) via UV–visible spectrophotometry corroborated this finding. Ultimately, the equilibrium concentration (Q_e) derived from the quasi-second-order adsorption kinetic model closely matched the experimental adsorption data. This alignment affirms the model's precision in accurately depicting the adsorption process (Table 2).

COD adsorption by both conventional and modified magnetic seeds displayed an ascending trajectory as the COD concentration increased. However, at a certain COD concentration threshold, the equilibrium adsorption amount attained a steady state. Furthermore, for equivalent COD concentrations, the adsorption efficiency of the

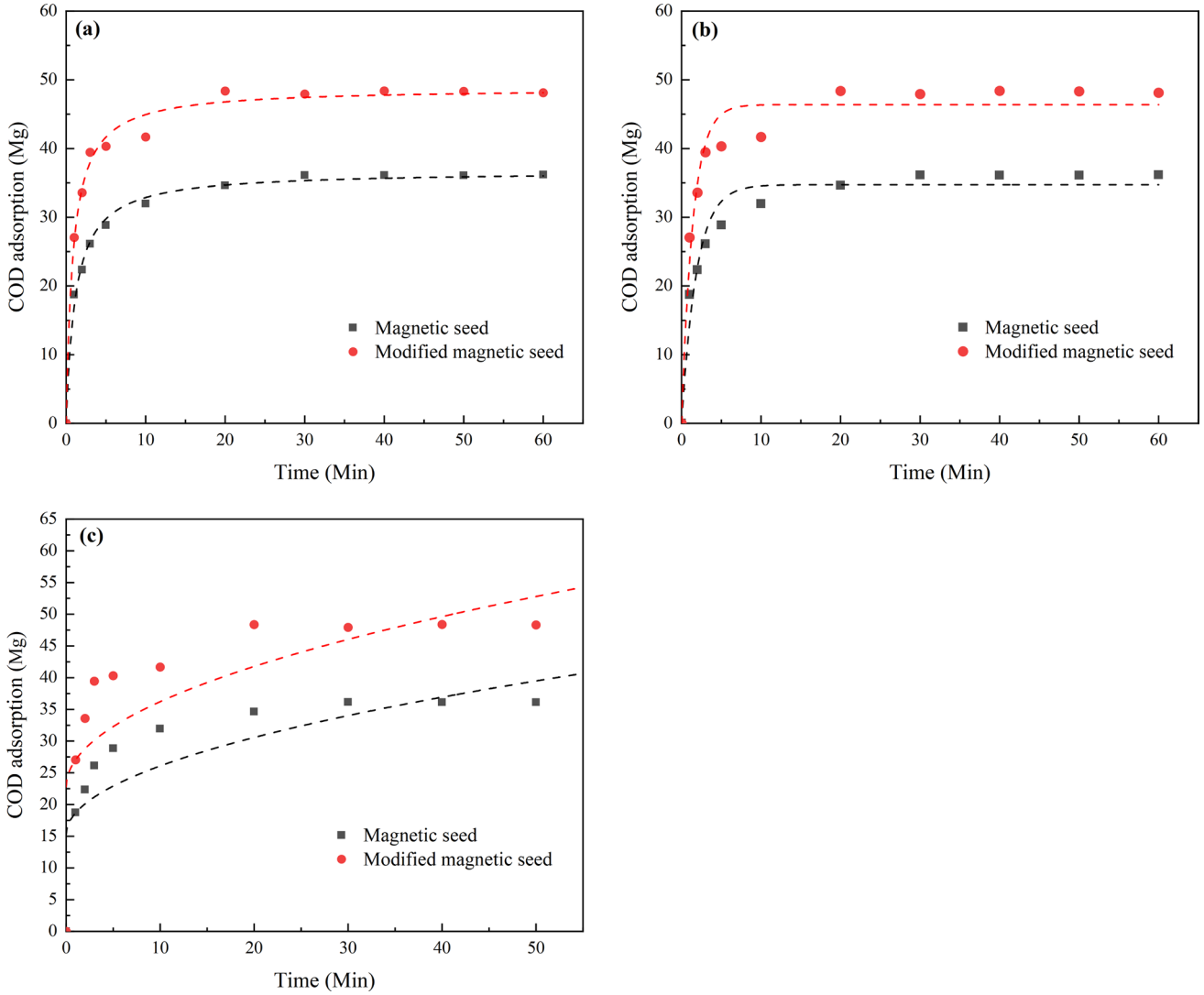

Fig. 5 Quasi-first-order adsorption kinetic model (**a**), quasi-second-order adsorption kinetic model (**b**), and internal diffusion adsorption kinetic model (**c**) (COD)

modified magnetic seeds significantly outperformed that of the conventional magnetic seeds, showcasing a superior adsorption capacity (Fig. 6a, b).

The Langmuir adsorption isotherm model and the Freundlich adsorption isotherm model effectively captured the adsorption behaviors of both conventional and modified magnetic seeds across varying COD concentrations. For the common magnetic seeds, the R^2 values for the Langmuir and Freundlich models were 0.96 and 0.89, respectively. Correspondingly, the modified magnetic seeds displayed R^2 values of 0.97 and 0.91. Notably, the saturation capacity of the modified magnetic seeds, as determined by the Langmuir adsorption isotherm model, measured 47.6 mg/g. This capacity surpassed that of the conventional magnetic seeds, which registered 34.3 mg/g, by an impressive 38.78% (Table 3).

Oil adsorption experiments

In the oil adsorption process by the magnetic seeds, there was a rapid initial increase in adsorption within the first 5 min, followed by a gradual decrease in adsorption rates from 5 to 15 min. Beyond the 15-min mark, adsorption continued, ultimately reaching saturation as the magnetic seeds became saturated with oil contaminants. In contrast, the modified magnetic seeds exhibited a faster adsorption rate, continuously accumulating oil contaminants from 5 to 12 min until saturation was achieved. By the 12-min mark, the surface of the modified magnetic seeds was nearly

Table 2 Parameters related to quasi-first-order adsorption kinetic model, quasi-second-order adsorption kinetic model, and internal diffusion model (COD)

Magnetic type	Experimental adsorption capacity	Quasi-first-order model adsorption kinetic model			Quasi-second-order adsorption kinetic model			Kinetic model of internal diffusion adsorption	
	mg	R^2	Q_e	K_1	R^2	Q_e	K_2	R^2	K_3
Magnetic seeds	36.15	0.93	34.70	0.533	0.97	36.7	0.023	0.64	3.4
Modified magnetic seeds	48.37	0.95	46.36	0.70	0.99	48.8	0.024	0.56	4.2

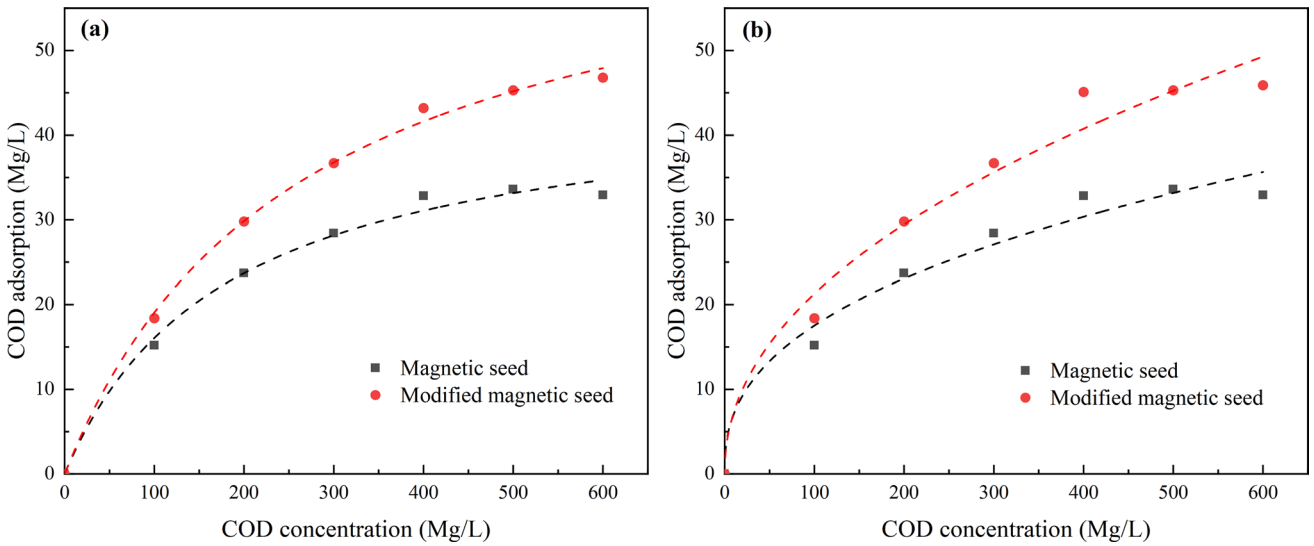

Fig. 6 Langmuir isotherm model (**a**) and Freundlich isotherm model (**b**) (COD)

Table 3 Parameters related to Langmuir isotherm model and Freundlich isotherm model (COD)

Magnetism	Langmuir			Freundlich		
	Q_m	b	R^2	K_f	n	R^2
Magnetic seeds	34.3	0.005	0.96	2.831	2.52	0.90
Modified magnetic seeds	47.6	0.004	0.99	2.461	2.13	0.92

entirely coated by oil contaminants, marking the conclusion of the adsorption process within this timeframe. Comparison of adsorption levels within the same time frame showcased a higher adsorption capacity of the modified magnetic seeds for petroleum, consistent with the earlier findings on COD adsorption. This emphasizes the conspicuous enhancement in petroleum adsorption capabilities demonstrated by the modified magnetic seeds (Fig. 7a–c).

The internal diffusion adsorption kinetic model yielded R^2 values of 0.85 for conventional magnetic seeds and 0.77 for modified magnetic seeds in the oil adsorption process. This discrepancy between observed behavior and the model's trend line suggests its inadequate representation of the intricate oil adsorption process. Conversely, the quasi-first-order adsorption kinetic model displayed higher R^2 values of 0.91 and 0.94 for the oil adsorption process by magnetic seeds. Upon employing the quasi-second-order adsorption kinetic model, the R^2 values escalated to 0.96 and 0.98 for conventional and modified magnetic seeds, respectively. Moreover, the equilibrium adsorption capacities predicted by these models (2.45 mg and 3.33 mg) closely approximated the experimental equilibrium adsorption quantities. This alignment further validates the quasi-second-order adsorption kinetic model's accuracy in characterizing the oil adsorption process for both conventional and modified magnetic seeds (Table 4).

The adsorption of oil by both conventional and modified magnetic seeds exhibited an augmentation with increasing oil concentration. However, an equilibrium adsorption capacity plateau was observed as the oil concentration reached a certain threshold. Notably, the modified magnetic seeds consistently outperformed the ordinary

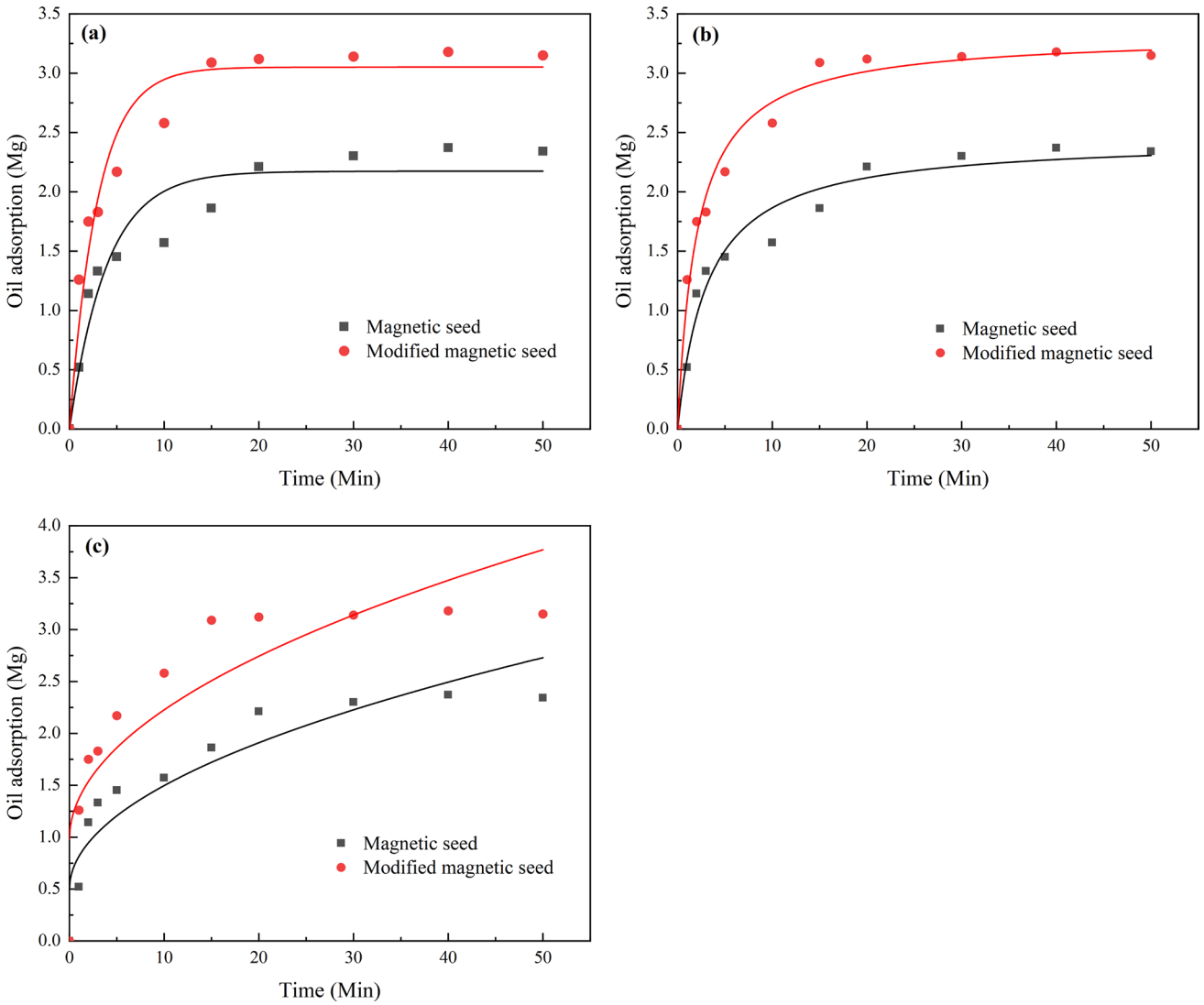

Fig. 7 Quasi-first-order adsorption kinetic model (**a**), quasi-second-order adsorption kinetic model (**b**), and kinetic model of internal diffusion adsorption (**c**) (oil)

magnetic seeds in terms of adsorption capacity and effectiveness (Fig. 8a, b).

The Langmuir adsorption isotherm model was utilized to model fats and oils adsorption by magnetic seeds at various concentrations, resulting in R^2 values of 0.95 and 0.96, respectively. Similarly, the Freundlich adsorption isotherm model demonstrated R^2 values of 0.98 and 0.99, respectively. The n value in the Freundlich adsorption isotherm model signifies the adsorbent's binding capacity, with higher n values indicating enhanced adsorption potential. In this study, the n values obtained from the Freundlich model were 1.312 for conventional magnetic seeds and 1.661 for modified magnetic seeds. These values denote favorable oil adsorption tendencies for both ordinary and modified magnetic seeds. However, the higher n value for modified magnetic seeds signifies a more robust adsorption capacity compared to the conventional seeds (Table 5).

Impact of various dosing combinations

When relying solely on flocculant PAC to treat oilfield-produced water, the removal efficiency for both oil and COD is least effective during a 5-min settling period. This inefficiency can be attributed to the limited flocculation effect within this short timeframe, as it falls short of achieving optimal settling conditions. However, a significant enhancement in both oil and COD removal rates is observed upon the introduction of PAM and magnetic seeds. The introduction of PAM notably improves the removal rates by optimizing flocculation conditions. Acting as a coagulation aid, PAM enhances the effectiveness

Table 4 Parameters related to quasi-first-order, quasi-second-order, and internal diffusion adsorption kinetic models (oil)

Magnetic type	Experimental adsorption capacity	Quasi-first-order model adsorption kinetic model			Quasi-second-order adsorption kinetic model			Kinetic model of internal diffusion adsorption	
	mg	R^2	Q_e	K_1	R^2	Q_e	K_2	R^2	K_3
Magnetic seeds	2.3	0.91	2.17	0.256	0.96	2.45	0.130	0.85	0.315
Modified magnetic seeds	3.2	0.94	3.05	0.337	0.98	3.33	0.145	0.77	0.395

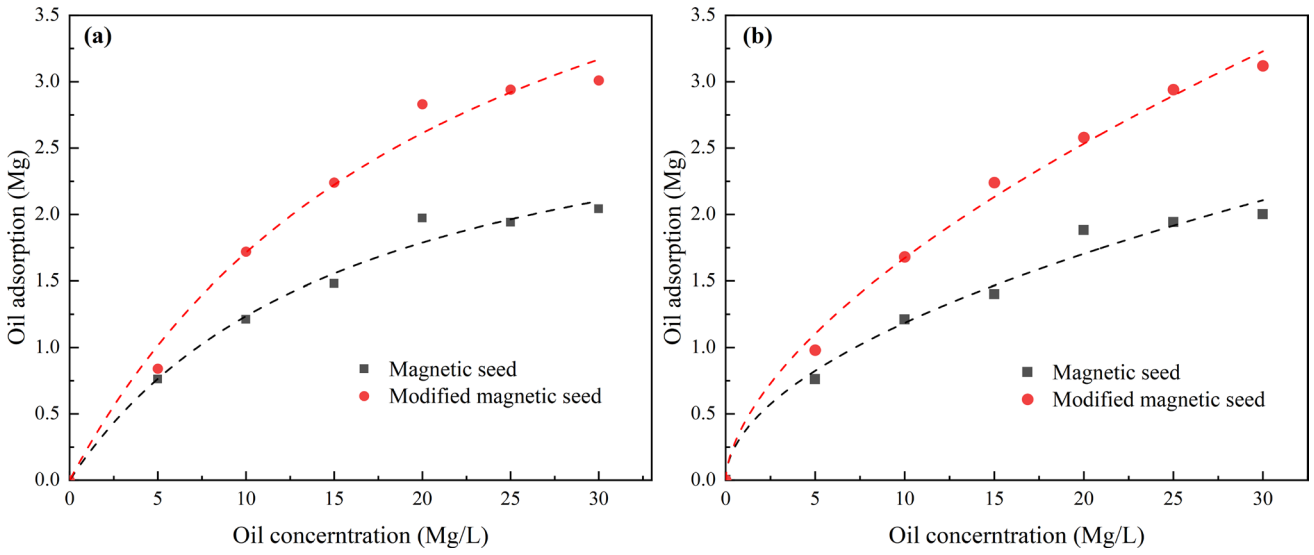

Fig. 8 Langmuir isotherm model (**a**) and Friedrich isotherm model (**b**) (oil)

Table 5 Langmuir isotherm model- and Freundlich isotherm model-related parameters (oil)

Magnetism	Langmuir			Freundlich		
	Q_m	b	R^2	K_f	n	R^2
Magnetic seeds	2.42	0.062	0.95	2.211	1.312	0.98
Modified magnetic seeds	3.38	0.045	0.96	2.042	1.661	0.99

of flocculation and improves the structure of pollutant flocs. This leads to larger and denser pollutant flocs, thereby improving removal efficiency. Simultaneously, the magnetic seeds, with their ionic polarity, metallic properties, and strong adsorption capacity, act as effective carriers for pollutants. This strengthens the binding of pollutants, leading to the formation of denser and heavier flocs, consequently enhancing flocculation and sedimentation efficiency. To further optimize the treatment efficacy of oilfield-produced water, a dosing combination of PAC + modified magnetic seeds + PAM was adopted, aiming to maximize the synergistic effects of these components (Fig. 9).

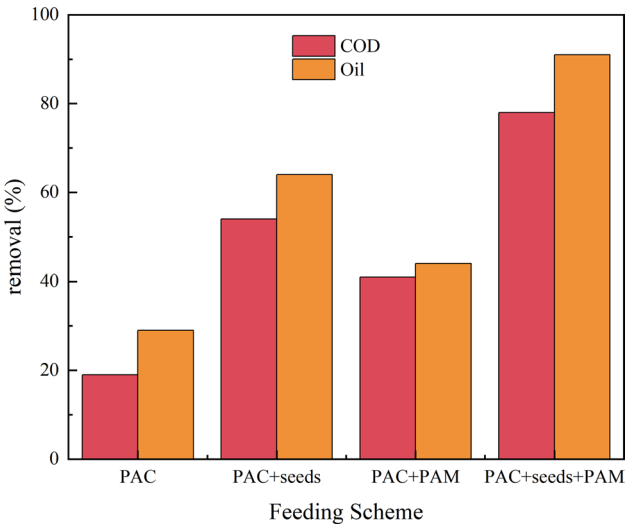

Fig. 9 Effect of dosing regimen on oil and COD removal

Dosage influence

The removal efficiency of both COD and petroleum increases proportionally with higher magnetic seed dosing. Upon reaching a peak removal efficiency, continued dosing of magnetic seeds results in an equilibrium removal rate. Optimal results are achieved with a dosage of 4g of ordinary magnetic seeds, leading to a reduction in COD concentration from 1527 to 632.6 mg/L (a removal rate of 58.6%) and a decline in oil concentration from 63 to 18.54 mg/L (a removal rate of 71%). Similarly, the best performance for modified magnetic seeds is observed at a dosage of 3 g, resulting in a COD concentration of 394.3 mg/L (a removal rate of 58.6%) and an oil concentration of 4.1 mg/L (a removal rate of 71%). The reason for this phenomenon is that the increase in magnetic seed dosage provides more carriers for pollutant flocs, allowing these flocs to adhere to the magnetic seed surfaces and aiding swift removal through sedimentation. This mechanism significantly enhances the treatment efficiency for COD and petroleum. The existing literature suggests that as magnetic seed concentration increases, Zeta potential rises, impacting the compression of the double electric layer in flocculation. This emphasizes the complex interplay of factors affecting flocculation efficacy. Moreover, the superior performance of surface-modified magnetic seeds in treating oily wastewater compared to their ordinary counterparts can be attributed to the irregular surface and finer pores of the former. These features result in a larger specific surface area, enhancing pollutant adsorption and consequently elevating COD and oil removal rates (Su et al. 2016; Liu et al. 2016; Sun at al. 2016) (Fig. 10a, b).

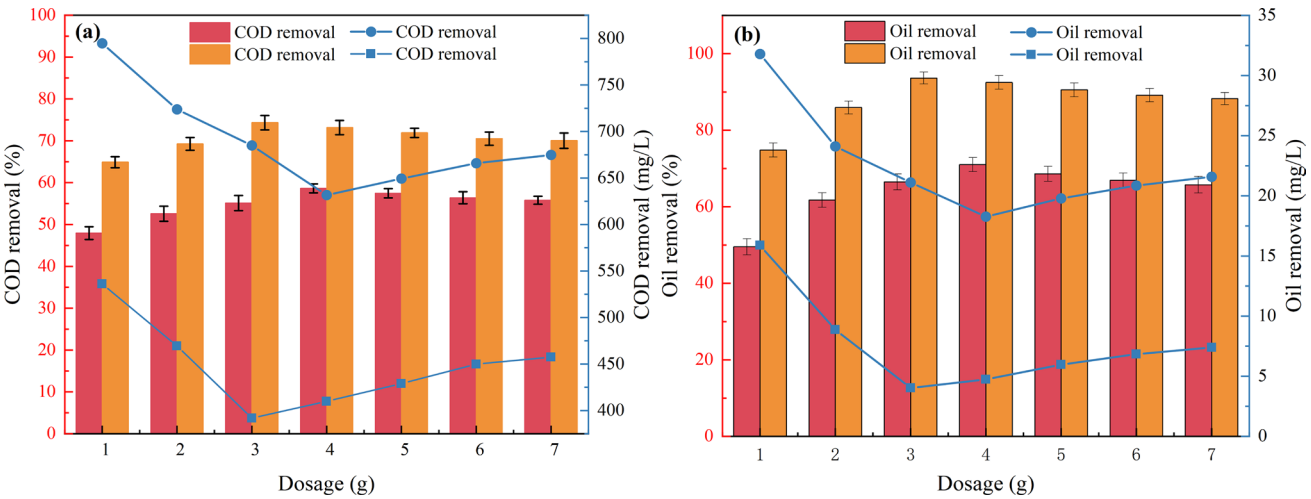

Fig. 10 Effect of magnetic seed dosing on COD removal (**a**) and effect of magnetic seed dosing on oil removal (**b**)

PAC influence

As the dosing concentration of flocculant PAC increased, both the removal rates of COD and petroleum showed a corresponding increase. The most effective removal rates for COD by both magnetic seeds and modified magnetic seeds were achieved at a flocculant concentration of 250 mg/L. This resulted in a reduction of COD concentration from 1527 to 621.7 mg/L and 391.6 mg/L, corresponding to removal rates of 59.3% and 74.4%, respectively. Similarly, the optimal petroleum removal was achieved at a flocculant concentration of 200 mg/L. Under this condition, petroleum concentration was reduced from 63 to 17.3 mg/L and 3.1 mg/L, yielding removal rates of 72.5% and 95.1%, respectively. This result directly stems from the mechanism of flocculation. The introduction of the flocculant initiates the adsorption of hydroxyl groups onto colloidal particles in water, facilitating complementary coordination, bridging, and anisotropic charge neutralization. Consequently, this process leads to the formation of Al $(OH)_3$ colloidal precipitates, fostering collisional bonding among colloidal particles (Ganjidoust et al. 1996). At lower PAC concentrations, the flocculant's positive ions neutralize the negative charges on pollutants. However, this might not yield flocs of sufficient size and gravity to overcome buoyancy, hampering effective sedimentation (Zheng et al. 2011). Therefore, it is suspended on the surface of the solution; at the same time, the low concentration of flocculant cannot fully net and sweep the pollutants in the water, and the adsorption and bridging effect between flocculant and colloidal particles is also inhibited. Higher concentrations of the flocculant are essential to ensure adequate netting and sweeping of pollutants, enabling effective adsorption bridging between the flocculant and colloidal particles (Jia et al. 2017). Nevertheless, excessive concentrations of the flocculant result in an abundance of positively charged particles, intensifying repulsion and destabilizing the system (Jia et al. 2018; Chen et al. 2016; Zagklis et al. 2012). Optimal treatment efficacy for both COD and petroleum pollutants is achieved with a flocculant concentration of 250 mg/L in magnetic flocculation (Fig. 11a, b).

PAM influence

Increasing the dosing concentration of coagulant PAM resulted in higher removal rates of both COD and petroleum. Optimal treatment efficacy was observed for both ordinary and modified magnetic seeds at a coagulant concentration of 2 mg/L. In this scenario, COD concentration decreased from 1621 to 647.4 mg/L and 377.1 mg/L, corresponding to removal rates of 57.6% and 75.3%, respectively. Petroleum concentration decreased from 63 to 19.6 mg/L and 4.9 mg/L, with removal rates of 68.8% and 92.3%, respectively. The introduction of PAM as a polymer coagulant aid rapidly forms large-sized pollutant flocs with multiple branches, enhancing adsorption and bridging capabilities. This augmentation strengthens flocculation, reducing COD and oil concentrations. Experiments indicate that coagulant aids accelerate flocculation speed by increasing the rotation radius of high-molecular-weight PAM in water. This larger radius facilitates faster collision and adsorption of impurity particles with PAM, expediting flocculation. However, excessive PAM dosage stabilizes unstable impurity particles in water, undermining treatment effectiveness. Moreover, PAM, being a macromolecule organic matter, has inherent toxicity and potential for pollution. While it enhances treatment effectiveness, it may lead to secondary pollution. Residual monomer content in oily and municipal sewage

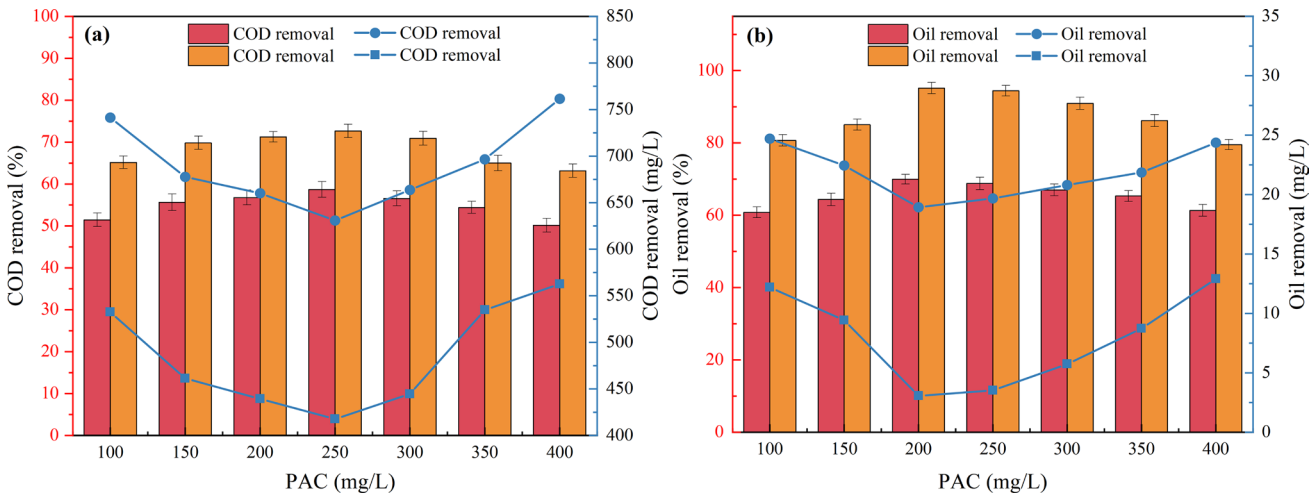

Fig. 11 Effect of PAC on COD removal (**a**) and effect of PAC on oil removal (**b**)

treatments typically remains below 1%, limiting PAM use in water treatment. Consequently, researchers are exploring new, pollution-free flocculants for enhanced water treatment (Raj et al. 2016; Chao aet al. 2015) (Fig. 12a, b).

pH influence

Both COD and petroleum removal rates increased with rising pH levels. The optimal removal rates for petroleum and COD using common magnetic seeds were achieved within a pH range of 7–8. Specifically, COD concentration decreased from 1527 to 621.4 mg/L and 386.4 mg/L, with corresponding removal rates of 59.3% and 74.7%. Similarly, petroleum concentration decreased from 63 to 17.7 mg/L and 4.2 mg/L, yielding removal rates of 71.9% and 93.3%. This phenomenon can be attributed to the strong electroneutralization-coagulation mechanism of the hydrolysis product-polynuclear hydroxyl polymer, existing in a high-valence form (Yang and Ni 2012; Guerin et al. 2017). The range of pH 7 to 8 results in optimal flocculation efficacy due to two key factors:

Influence of pH on aluminum ion hydrolysis and polymerization

PAC ionizes in water to generate Al^{3+} ions, but the basic Al^{3+} ions do not exist in the solution, but often exist in the form of hydrated ions of Al $(H_2O)_6{}^{3+}$. As the pH continues to increase, OH- ligands will continue to replace hydrated aluminum ions-coordinated water molecules, and the hydrolysis process and polymerization process occur almost simultaneously. As shown in the following equation, the final product is a precipitate of $[\{Al(OH)_2\}nAl]^{n+3+}$. As pH increases, hydroxyl ions (OH^-) replace coordinated water molecules of hydrated aluminum ions ($Al(H_2O)_6{}^{3+}$), promoting hydrolysis and polymerization reactions. It is confirmed that pH value is one of the important factors in the removal of organic pollutants (Olukowi et al. 2022).

$$Al\left(H_2O\right)_6^{3+} + H_2O \leftrightarrow Al\left(H_2O\right)_5OH^{2+} + H_3O^+$$

$$Al\left(H_2O\right)_5OH^{2+} \rightarrow Al\left(H_2O\right)_4(OH)_2^+ \rightarrow Al\left(H_2O\right)_3(OH)_3 \rightarrow Al\left(H_2O\right)_2(OH)_4^- \rightarrow$$

$$Al\left(H_2O\right)(OH)_5^{2-} \rightarrow Al(OH)_6^{3-}$$

$$2AlOH^{2+} \rightarrow \left[Al(OH)_2Al\right]^{4+} \rightarrow \left[Al(OH)_2Al(OH)_2Al\right]^{5+} \rightarrow \cdots\cdots \rightarrow \left[\{Al(OH)_2\}_nAl\right]^{n+3+}$$

Effect of pH on solubility of $Al(OH)_3$, a hydrolysis product of Al^{3+}

The hydrolysis product of $Al_3{}^+$, $Al(OH)_3$, exhibits different forms at varying pH levels. Previous studies by Matijevic, Brosset, and others confirm that $Al(OH)_3$ primarily precipitates within the pH range of 6–8. As pH increases beyond 8, part of $Al(OH)_3$ dissolves into $Al(OH)_4{}^-$. The content of $Al(OH)_3$ significantly influences flocculation efficacy. Thus, the optimal treatment effect occurs at a pH range of 6 to 8, as corroborated by experimental results (Fig. 13 a, b). In addition, the pH will also have a corresponding impact on the coagulant PAM. The polymer chain of PAM is the key to adsorption and bridging. When the pH is too small or too high, the polymer bonds will break and curl, thus affecting the bridging. The effect and distance reduce the flocculation effect.

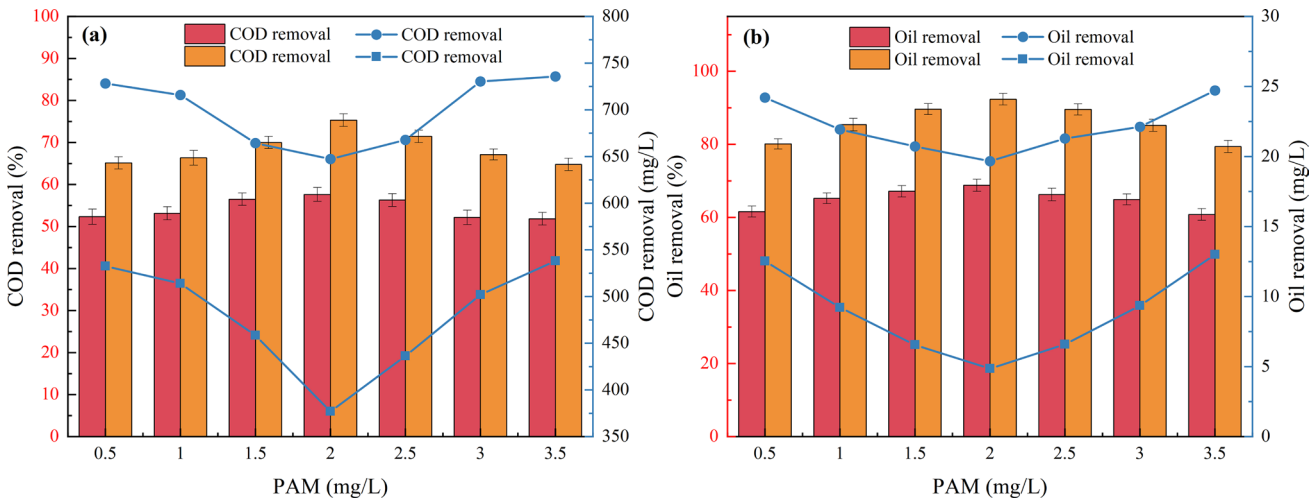

Fig. 12 Effect of PAM on COD removal (**a**) and effect of PAM on oil removal (**b**)

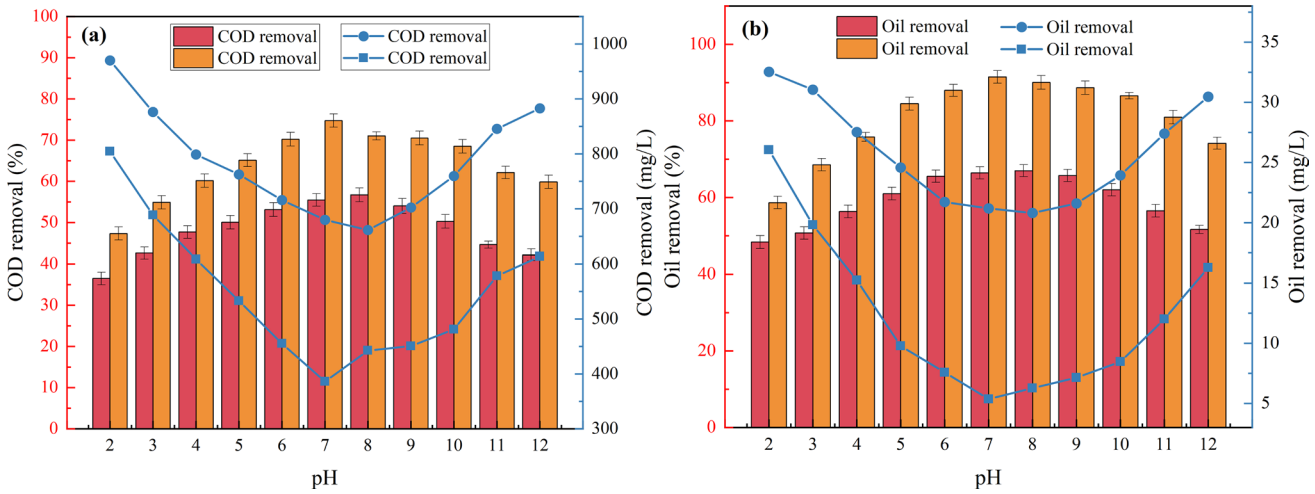

Fig. 13 Effect of pH on COD removal (**a**) and effect of pH on oil removal (**b**)

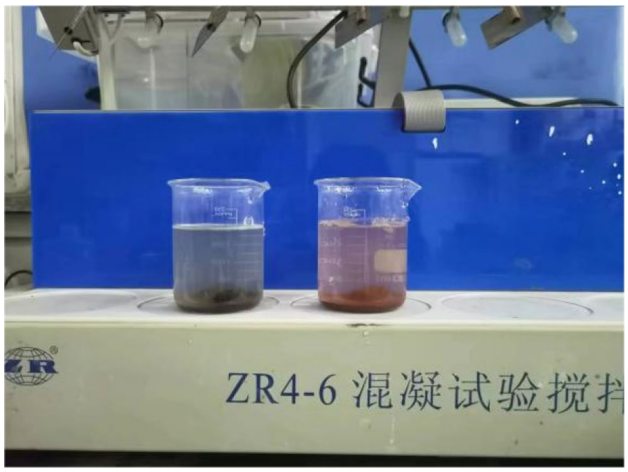

Fig. 14 Water sample after magnetic flocculation treatment

Results under optimal conditions

The optimal conditions for the magnetic flocculation treatment stage were established through one-factor experiments: a magnetic flocculation flocculant PAC concentration of 250 mg/L, a magnetic seed dosage of 4 g, a coagulant PAM concentration of 2 mg/L, a water temperature of 20–25 ℃, pH ranging from 7 to 8, and a settling time of 7 min for magnetic flocculation using ordinary magnetic seeds. For magnetic flocculation treatment with modified magnetic seeds, the optimal conditions included a magnetic flocculation flocculant PAC concentration of 250 mg/L, a magnetic seed dosage of 3 g, a coagulant PAM concentration of 2 mg/L, a water temperature of 20–25 °C, a pH range of 7–8, and a settling time of 6 min (Fig. 14).

Through magnetic flocculation, the treatment of oily wastewater resulted in a reduction of the average COD concentration from 1527 to 614.8 mg/L and 374.3 mg/L, leading to removal rates of 59.7% and 75.5%, respectively. Furthermore, the average oil concentration decreased from 63 to 18.3 mg/L and 4.3 mg/L, corresponding to removal rates of 71% and 93.2%, respectively. These results highlight the notable advantages of modified magnetic seeds over ordinary magnetic seeds in the treatment of oily wastewater (Table 6). It is important to note that, as shown in (Table 7), the maximum adsorption capacity is much higher than previously reported values for adsorbents.

Conclusion

In conclusion, this study investigated the treatment of oily wastewater through magnetic flocculation utilizing modified magnetic seeds. The key findings are as follows:

Surface morphology analysis Ordinary magnetic seeds exhibited a predominantly spherical shape with small particle size and a smooth surface. In contrast, modified magnetic seeds displayed irregular lumps with non-uniform particle sizes and a rough surface.

Adsorption mechanism The study revealed that modified magnetic seeds possessed superior adsorption capacity and faster equilibrium rates for both COD and petroleum compared to ordinary magnetic seeds. The Langmuir and Freundlich adsorption isotherm models accurately characterized the adsorption behaviors of both magnetic seed types on COD. The Langmuir model demonstrated a 38.78% higher saturated adsorption capacity for modified magnetic seeds (47.6 mg/g) compared to ordinary magnetic seeds (34.3 mg/g). The oil adsorption analysis revealed

Table 6 Experimental results under optimal conditions

Number of experiments	1 time	2 times	3 times	Average value
Magnetic seeds				
COD after treatment (mg/L)	624.3	608.0	612.0	614.8
COD removal (%)	59.1%	60%	59.9%	59.7%
Oil concentration after treatment (mg/L)	18.6	17.3	18.9	18.3
Oil removal rate (%)	70.4%	72.5%	70%	71%
Modified magnetic seeds				
COD after treatment (mg/L)	384.5	372.1	366.4	374.3
COD removal (%)	74.8%	75.6%	76%	75.5%
Oil concentration after treatment (mg/L)	4.1	4.6	4.2	4.3
Oil removal rate (%)	93.5%	92.7%	93.3%	93.2%

Table 7 Adsorption capacities of various adsorbents for the adsorption of oily sewage

Adsorbents	Adsorption time (h)	Maximum adsorption capacities (mg/g) (%)	Refs.
Surface-modified magnetic Fe_3O_4	0.1	93.2	This work
Amphiphilic chitosan derivative	0.1	95	Sun et al. (2008)
Surfactant-modified sepiolite	1.5	74.7	Li et al. (2018)
GO powder	0.2	90	Diraki et al. (2019)
Phragmites australis	2.0	91.32	El Shahawy and Heikal (2018)
Modified date seeds	2.0	53.3	Al Haddabi et al. (2015)
Ultra-light carbon foams	1.5	99	Yang et al. (2019)

that modified magnetic seeds exhibited larger adsorption capacity and quicker equilibrium compared to ordinary magnetic seeds, with the Freundlich adsorption isotherm model favorably describing the adsorption behaviors. The *n* values of 1.312 and 1.661 supported the enhanced adsorption capacity of modified magnetic seeds.

Optimal treatment program The combination of flocculant (PAC) + magnetic seeds + coagulant aid (PAM) proved significantly superior to other combinations. The optimal conditions for magnetic flocculation with modified magnetic seeds included a magnetic flocculation flocculant PAC concentration of 250 mg/L, a magnetic seed dosage of 3 g, a coagulant aid PAM concentration of 2 mg/L, a water temperature of 20–25 °C, pH ranging from 7 to 8, and a settling time of 6 min.

Enhanced effectiveness Under the established optimal conditions, magnetic flocculation utilizing modified magnetic seeds achieved remarkable results. It led to a COD removal rate of 75.5%, reducing the concentration from 1527 to 374.3 mg/L, and a remarkable 93.2% removal of oil pollutants, lowering the concentration from 63 to 4.3 mg/L. By contrast, magnetic flocculation with ordinary magnetic seeds achieved a 59.7% COD removal (from 1527 to 614.8 mg/L) and a 71% oil removal (from 63 to 18.3 mg/L). These outcomes underscore the efficacy of magnetic flocculation in treating oily sewage.

Acknowledgements The authors would like to thank Nitrogen Conversion Mechanism of Feammox Process Based on NDFO Iron Oxide Biocycle in Applied Basic Research Program of Liaoning Provincial Science and Technology Department.

Author's contribution All authors contributed to the study conception and experiment design. Interpretation of data from material characterization tests was performed by BW and QZ. All authors read and approved the final manuscript.

Funding The work was financially supported by Research on Nitrogen Conversion Mechanism of Feammox Process Based on NDFO Iron Oxide Biocycle in Applied Basic Research Program of Liaoning Provincial Science and Technology Department (2022JH2/101300120), 151536.54RMB.

Data availability The author's confirm that the data supporting the findings of this study are available within the article. Raw data that support the findings of this study are available from the corresponding author, upon reasonable request.

Declarations

Conflict of interest The authors declare no conflict of interest.

References

Al Haddabi M, Vuthaluru H, Znad H, Ahmed M (2015) Removal of dissolved organic carbon from oily produced water by

adsorption onto date seeds: equilibrium, kinetic, and thermodynamic studies. Water Air Soil Pollut 226:1
Chao Y, Liang WY, Liu LJ, Li FZ, Fan QL, Sun XL (2015) Harvesting chlorella vulgaris by magnetic flocculation using Fe_3O_4 coating with polyaluminium chloride and polyacrylamide. Bioresour Technol 198:789–796
Chen YQ, Luo M, Cai WF (2016) Influence of operating parameters on the performance of magnetic seeding flocculation. Environ Sci Pollut Res 23:2873–2881
Diraki A, Mackey HR, McKay G, Abdala A (2019) Removal of emulsified and dissolved diesel oil from high salinity wastewater by adsorption onto graphene oxide. J Environ Chem Eng 7(1):03106
El Shahawy A, Heikal G (2018) Organic pollutants removal from oily wastewater using clean technology economically, friendly biosorbent (*Phragmites australis*). Ecol Eng 122:207–218
Elamin NY, Modwi A, Abd El-Fattah W, Rajeh A (2022) Synthesis and structural of Fe_3O_4 magnetic nanoparticles and its effect on the structural optical, and magnetic properties of novel poly(methyl methacrylate)/polyaniline composite for electromagnetic and optical applications. Opt Mater 135:113323
Farahat MM, Khalek MAA, Sanad MMS (2022) Affordable and reliable cationic-anionic magnetic adsorbent: processing characterization, and heavy metals removal. J Clean Prod 360:132178
Ganjidoust H, Tatsumi K, Wada S, Kawase M (1996) Role of peroxidase and chitosanin removing chlorophenols from aqueous solution. Water Sci Technol 34:151–159
Guerin L, Coufort-Saudejaud C, Line A, Frances C (2017) Dynamics of aggregate size and shape properties under sequenced flocculation in a turbulent Taylor–Couette reactor. J Colloid Interface Sci 172(491):167–178
Hong MK, Park BJ, Choi HJ (2007) Preparation and physical characterization of polyacrylamide coated magnetite particles. Phys Status Solidi A 204:4182–4185
Jia H, Yang G, Ngo HH, Guo WS, Zhang HW, Gao F, Wang J (2017) Enhancing simultaneous response and amplification of biosensor in microbial fuel cell-based upflow anaerobic sludge bed reactor supplemented with zero-valent iron. Chem Eng J 327:1117–1127
Jia H, Liu WB, Wang J, Ngo HH, Guo WS, Zhang HW (2018) Optimization of sensing performance in an integrated dual sensors system combining microbial fuel cells and upflow anaerobic sludge bed reactor. Chemosphere 210:931–940
Jiang C, Wang R, Ma W (2010) The effect of magnetic nanoparticles on Microcystis aeruginosa removal by a composite coagulant. Colloids Surf A 369:260–267
Langmuir I (1918) The adsorption of gases on plane surfaces of glass, mica and platinum. J Am Chem Soc 40:1361–1403
Li XB, Liu JT, Wang YT, Xu HX, Cao YJ, Deng XW (2015) Separation of oil from wastewater by coal adsorption-column flotation coal adsorption-flotation columns separate oil from wastewater. Sep Sci Technol 50:583–591
Li YF, Wang MX, Sun DJ, Li YJ, Wu T (2018) Effective removal of emulsified oil from oily wastewater using surfactant-modified epiolite. Appl Clay Sci 157:227–236
Li YF, Zimmerman AR, He F, Chen JJ, Han LJ, Chen H, Hu X, Gao B (2020) Solvent-free synthesis of magnetic biochar and activated carbon through ball-mill extrusion with Fe_3O_4 nanoparticles for enhancing adsorption of methylene blue. Sci Total Environ 722:137972
Liu XW, Hu QY, Fang Z, Zhang XJ, Zhang BB (2009a) Magnetic chitosan nanocomposites: a useful recyclable tool for heavy metal ion removal. Langmuir 25:3–8
Liu D, Li FT, Zhang BR (2009b) Removal of algal blooms in freshwater using magnetic polymer. Water Sci Technol 59(1085):1091
Liu D, Wang P, Wei GR, Dong WB, Hui F (2013) Removal of algal blooms from freshwater by the coagulation-magnetic separation method: coagulation-magnetic separation to remove freshwater red tides. Environ Sci Pollut Res 20:60–65
Liu PR, Zhang HL, Wang T, Yang WL, Hong Y, Hou YL (2016) Functional graphene-based magnetic nanocomposites as magnetic flocculant for efficient harvesting of oleaginous microalgae. Algal Res 19:86–95
Liu Y, Yang J, Jiang WM, Chen YM, Yang CJ, Wang TY, Li XY (2018) Experimental studies on the enhanced performance of lightweight oil recovery using a combined electrocoagulation and magnetic field processes. Chemosphere 205:601–609
Ma M, Zhang Y, Yu W, Shen HY, Zhang HQ, Gu N (2003) Preparation and characterization of magnetite nanoparticles coated by amino silane. Colloids Surf A 212:219–226
Njoku VO, Islam MA, Asif M, Hameed BH (2014) Preparation of mesoporous activated carbon from coconut frond for the adsorption of carbofuran insecticide. J Anal Appl Pyrolysis 110:172–180
Olukowi OM, Xie Y, Zhou ZY, Adebayo IO, Zhang YJ (2022) Performance improvement and mechanism of composite PAC/PDMDAAC coagulant via enhanced coagulation coupled with rapid sand filtration in the treatment of micro-polluted surface water. J Environ Chem Eng. https://doi.org/10.1016/j.jece.2022.108450
Panda SK, Aggarwal I, Kumar H, Prasad L, Kumar A, Sharma A, Vo DVN, Thuan DV, Mishra V (2021) Magnetite nanoparticles as sorbents for dye removal: a review. Environ Chem Lett 19:2487–2525
Pinto J, Athanassiou A, Fragouli D (2018) Surface modification of polymeric foams for oil spills remediation. J Environ Manag 206:872–889
Raj P, Batchelor W, Blanco A, de la Fuente E, Negro C, Garnier G (2016) Photocatalytic reduction of carbon dioxide to methanol using nickel-loaded TiO_2 supported on activated carbon fiber. J Colloid Interface Sci 481:158–167
Sharma A, Lee BK (2017) Photocatalytic reduction of carbon dioxide to methanol using nickel-loaded TiO_2 supported on activated carbon fiber. Catal Today 298:158–167
Shen YF (2022) Preparation of renewable porous carbons for CO2 capture—a review. Fuel Process Technol. https://doi.org/10.1016/j.fuproc.2022.107437
Shin KY, Hong JY, Jang J (2011) Heavy metal ion adsorption behavior in nitrogen-doped magnetic carbon nanoparticles: isotherms and kinetic study. J Hazard Mater 190:36–44
Singh G, Lee JM, Kothandam G, Palanisami T, Al-Muhtaseb AH, Karakoti A, Yi JB (2021) A review the synthesis and applications of nanoporous carbons for the removal of complex chemical contaminants. Bull Chem Soc Jpn 94:1232–1257
Su ZY, Li X, Yang YL, Xu ML, Ding YX, Zhou ZW (2016) Optimization of magnetic-seeding coagulation in artificially polluted surface water treatment by response surface methodology. Desalin Water Treat 57:20671–20682
Sun GZ, Chen XG, Li YY, Liu CS, Liu CG, Zheng B, Gong ZH, Sun JJ, Chen H, Li J, Lin WX (2008) Preparation and properties of amphiphilic chitosan derivative as a coagulation agent. Environ Eng Sci 25:1325–1332
Sun XT, Li Q, Yang LR, Liu HZ (2016) Removal of chromium (VI) from wastewater using weakly and strongly basic magnetic adsorbents: adsorption/desorption property and mechanism comparative studies. RSC Adv 6:18471–18482
Wang SK, Wang F, Hu YR, Stiles AR, Guo C, Liu CZ (2014) Magnetic flocculant for high efficiency harvesting of microalgal cells. ACS Appl Mater Interfaces 6:109–115
Wang YQ, Lin CY, Liu XT, Ren WB, Huang XK, He MC, Ouyang W (2021) Efficient removal of acetochlor pesticide from water using magnetic activated carbon: Adsorption performance, mechanism, and regeneration exploration. Sci Total Environ. https://doi.org/10.1016/j.scitotenv.2021.146353
Wang S, Wang H, Wang SX, Fu LK, Zhang LB (2023) Novel magnetic covalent organic framework for the selective and effective removal

of hazardous metal Pb (II) from solution: synthesis and adsorption characteristics. Sep Purif Technol. https://doi.org/10.1016/j.seppur.2022.122783

Yang XJ, Ni L (2012) Synthesis of hybrid hydrogel of poly(AM coDADMAC)/silica sol and removal of methyl orange from aqueous solutions. Chem Eng J 209:194–200

Yang S, Wang F, Tang QG, Wang PF, Xu ZS, Liang JS (2019) Utilization of ultra-light carbon foams for the purification of emulsified oil wastewater and their adsorption kinetics. Chem Phys 516:139–146

Zagklis DP, Koutsoukos PG, Paraskeva CA (2012) A combined coagulation/flocculation and membrane filtration process for the treatment of paint industry wastewaters. Ind Eng Chem Res 51:15456–15462

Zhang B, Shi WX, Yu SL, Zhu YB, Zhang RJ, Tay JH (2019) Adsorption of anion polyacrylamide from aqueous solution by polytetrafluoroethylene (PTFE) membrane as an adsorbent: kinetic and isotherm studies. J Colloid Interface Sci 544:303–311

Zhao Y, Wang XY, Jiang XX, Fan QJ, Li X, Jiao LY, Liang WY (2018) Harvesting of *Chlorella vulgaris* using Fe_3O_4 coated with modified plant polyphenol. Environ Sci Pollut Res 25:26246–26258

Zheng HL, Zhu GC, Jiang SJ, Tshukudu T, Xiang XY, Zhang P, He QA (2011) Investigations of coagulation-flocculation process by performance optimization, model prediction and fractal structure of flocs. Desalination 269:148–156